Supplemental figure legends

Supplemental Figure 1. Functional TRPV1 expression in IEC and intestinal organoids. (A) PCR products generated with primers specific for *Trpv1-6* and *Gapdh* (housekeeping gene) after 30 cycles of amplification, corresponding to Q-PCR results presented **Figure 1A**. The mRNA was isolated from primary IEC samples and used for cDNA synthesis. **(B)** PCR products after 30 cycles of amplification of mRNA obtained from small intestinal organoids, corresponding to **Figure 1B**. **(C)** Expression of *Trpv1* transcripts in intestinal organoids and freshly isolated IEC, respectively, derived from WT and *Trpv1*$^{-/-}$ mice. *Cldn6* (claudin-6), an epithelial cell marker. *Gapdh*, housekeeping gene. **(D)** Expression of TRPV1 mRNA in human colorectal cancer cell lines (HCT116 and HCA-7) and rodent cell lines (rat small intestinal cell line, IEC-6; murine colorectal cancer cell line, CMT-93). Positive control: homogenates from mouse hippocampus (CNS). **(E)** Validation of anti-TRPV1 Abs for Western blotting with cell lysates from CHO^{K1} and TRPV1 overexpressing CHO^{TRPV1} cells. β-Actin: loading control. **(F)** Single cell suspensions of CHO^{K1} and CHO^{TRPV1} cells were stained with anti-TRPV1 Abs (red lines) and detected with rabbit anti-goat AF488 conjugate Abs (flow cytometry). IgG control: goat IgG (black lines). **(G)** Validation of functional TRPV1 activity recordings. CHO^{TRPV1} cells were loaded with 5 μM Fura-2 AM and $[Ca^{2+}]_{cyt}$ were measured in single cells during perfusion with PSS at room temperature (20 ˚C). **Left panel:** Stimulation with 1 nM capsaicin induced rapid $[Ca^{2+}]_{cyt}$ elevations. **Right panel:** Pretreatment of CHO^{TRPV1} cells with TRPV1 antagonist BCTC (1 μM) prevented $[Ca^{2+}]_{cyt}$ elevations induced by capsaicin (1 nM), but not ATP (10 μM). Mean ± SEM (n=52 for each condition). **(H)** Functional TRPV1 channel activity in the HCT116 cell line. Fura-2 loaded HCT116 cells were stimulated with increasing concentrations of capsaicin,

resulting in dose-dependent $[Ca^{2+}]_{cyt}$ increases (left panel). These capsaicin-induced Ca^{2+} responses were attenuated by pretreatment with TRPV1 antagonist BCTC (10 μM) (right panel).

Supplemental Figure 2. Functional effects of TRPV1 in IEC biology. (A) Gross crypt-villus architecture, Goblet cell and Paneth cell differentiation were unaffected in small intestines of *Trpv1*$^{-/-}$ mice. PAS staining (**top panels**) and immunostaining for matrix metalloprotease 7 MMP7 (**bottom panels**), respectively. **(B)** Numbers of Goblet cells and Paneth cells were similar in *Trpv1*$^{-/-}$ and WT intestinal organoids. Immunostaining of fixed organoids in Matrigel with AF488 conjugated wheat germ agglutinin (WGA) (**top panels**) or anti-MMP7 Abs (**bottom panels**), Phalloidin AF546 and DAPI and imaged by confocal fluorescent microscopy. **(C)** Capsaicin treatment inhibited ligand-induced $EGFR^{Tyr1068}$ phosphorylation. WT mice were pretreated with regular chow or capsaicin 0.01% (w/w) mixed in chow for 2 days and then treated with EGF (2 μg, i.p.) for 0 or 15 min. IEC lysates were analyzed by Western blotting. **(D)** WT mice received dietary capsaicin 0.01% (w/w) in chow or control chow for 4 weeks. Tissues were harvested and Ki67 staining with DAB detection of colon tissues was performed. Shown are representative pictures of colons used for Ki67 quantification. **(E)** Quantification of Ki67 positive cells of mice treated with dietary capsaicin or control diet (n=3 mice/group). **(F)** WT mice were treated with vehicle (EtOH), low dose capsaicin (0.3 mg/kg/day) or high dose capsaicin (3.0 mg/kg/day) for 5 consecutive days by gavage. Small intestinal tissues were harvested on day 5. Intestinal sections were stained with Alcian blue (counterstaining with nuclear fast red; **top panels**), or with anti-MMP7 Abs (counterstaining with hematoxylin; **bottom panels**). **(G)** Quantification of the area stained for mucin (Alcian blue) with ImageJ by using the Colour Deconvolution plugin (n=3 mice/group). **(H)** Quantification of the area

immunostained for MMP7 by immunohistochemistry with DAB (n=3 mice/group). Data are mean ± SEM. **P*<0.05 (t-test). Scale bars = 100 μm.

Supplemental Figure 3. Analysis of transgenic TRPV1^{IEC} mice. (A) Validation of conditional TRPV1 overexpression by PCR. Small intestinal and colonic IEC were harvested from TRPV1$^{fl/fl}$ and TRPV1^{IEC} (Cre positive) mice, together with spinal cord homogenates. PCR was performed for *Cre*, *Trpv1*, a neuronal cell marker (*Nefl;* Neurofilament), an epithelial cell marker (*Slc26a3*), and housekeeping gene *Gapdh.* The results showed endogenous expression of *Trpv1* in all tissues analyzed (TRPV1$^{fl/fl}$), whereas overexpression was only found in IEC lysates from Cre positive (TRPV1^{IEC}) mice. **(B)** Validation of conditional TRPV1 overexpression by Western blotting. Protein samples (IEC and spinal cord homogenates) were prepared for IB. Membranes were probed for TRPV1, a neuronal marker (Synaptophysin), an IEC marker (Occludin) and loading control β-Actin. TRPV1 overexpression was found only in IEC in Cre positive (TRPV1^{IEC}) mice. **(C)** Reduced IEC proliferation in colons from TRPV1^{IEC} mice. Representative pictures of Ki67+ cells in colon sections of TRPV1$^{fl/fl}$ and TRPV1^{IEC} mice are shown. **(D)** Quantification of Ki67+ cells in colons of TRPV1$^{fl/fl}$ and TRPV1^{IEC} mice, respectively. Data are shown as mean ± SEM (n=3). **(E)** RNA from colonic IEC isolated from TRPV1$^{fl/fl}$ and TRPV1^{IEC} mice were used for Q-PCR analysis for the expression of a proliferation marker, *Mki67*, normalized to *Gapdh*. Data are shown as mean ± SEM (n=3). **(F)** Reduced expression of a proliferation marker, *Mki67*, and EGFR target genes, *c-Fos*, *c-Jun* and *Egr1* in intestinal organoids generated from TRPV1^{IEC} mice. RNA from organoids was used for Q-PCR analysis, expression data was normalized to Gapdh. Mean ± SD (n=2). **(G)** Reduced staining intensity for

p-EGFR^{Y1068} in TRPV1^{IEC} compared to TRPV1$^{fl/fl}$ organoids. Scale bar = 100 μm. *P<0.05 (t-test) in D, E and F.

Supplemental Figure 4. Functional association between TRPV1 and EGFR signaling *in vitro*. (A) TRPV1 inhibits ligand-induced EGFR^{Y1068} phosphorylation. CHO^{K1} cells were transfected with empty vector, wt-EGFR, or wt-EGFR + TRPV1. Cells were then stimulated with 10 ng/mL EGF for indicated times, followed by Western blot analysis of total cell lysates. **(B)** Detailed time course of EGF-stimulated HCT116 cells transfected with empty vector or TRPV1. Total cell lysates were analyzed for multiple EGFR phospho-sites including Y992, Y1045, S1046/S1047, and Y1068 by Western blotting. TRPV1 overexpression suppressed Y992, Y1045, and Y1068 phosphorylation, whereas it potentiated phosphorylation of S1046/S1047. The S1046/S1047 residues are known to be phosphorylated by Ca^{2+}/calmodulin-dependent kinase II (CaMKII), suggesting activation of CaMKII by TRPV1 under these experimental conditions. Representative results of three independent experiments are shown. **(C)** Transfection of HCT116 cells with empty vector, TRPV3, or TRPV4-FLAG plasmids. Three days after transfection, cells were stimulated with EGF (1 ng/mL) and total cell lysates were analyzed by Western blotting for indicated proteins. **(D)** HCT116 cells were transfected with empty vector or TRPV5-GFP construct and analyzed by widefield fluorescent microscopy on day 3. **(E)** Mock or TRPV5-GFP transfected HCT116 cells were stimulated with EGF (1 ng/mL) followed by Western blot analysis of total cell lysates. Results are representative of three independent experiments.

Supplemental Figure 5. Physiological effects of TRPV1 signaling in intestinal organoids. **(A)** Enhanced TA zone in *Trpv1*$^{-/-}$ crypts in intestinal organoids. WT and *Trpv1*$^{-/-}$ organoids, as shown in **Figure 4E** (cropped, dotted lines), were generated from small intestines and cultured under similar conditions. Ki67 staining was performed 3 days after passing, together with Phalloidin AF546 and DAPI. Scale bars = 100 μm. **(B)** Ki67 staining of WT and *Trpv1*$^{-/-}$ organoids at the same growth stage by immunohistochemistry with DAB (brown) and hematoxylin counterstaining. Representative examples are shown. **(C)** Quantification of Ki67+ cells (%) relative to hematoxylin staining nuclei with ImageJ (ImmunoRatio plugin). Mean ± SEM (n=7). **P*<0.05 (t-test). **(D)** Proliferation in EGF-starved WT and *Trpv1*$^{-/-}$ organoids similar to those shown in **Figure 4, G and H** at lower magnification. Scale bars = 100 μm.

Supplemental Figure 6. Identification of PTP1B activity as a downstream effector mechanism of TRPV1. **(A)** Validation of the CaM inhibitor, W-7, as a blocker of the downstream CaMKII pathway. HCT116 cells were pretreated with 0 or 10 μM W-7 for 1 hr. Cells were then stimulated with 5 μM ionomycin for 0, 10, or 30 min. Total cell lysates were analyzed by Western blotting for p-CaMKII, total CaMKII, and β-actin. W-7 pretreatment efficaciously inhibited constitutive and ionomycin-induced CaMKII phosphorylation. **(B)** Calmodulin (CaM) does not play a role in TRPV1-mediated effects on EGFR signaling. HCT116 cells were transfected with control or TRPV1 plasmid, followed by stimulation with EGF (1 ng/mL) for indicated times. CHO^{K1} and CHO^{TRPV1} cells were transfected with control or wt-EGFR plasmid, followed by EGF stimulation as indicated. Pre-treatment with 10 μM W-7 (1 hr) before stimulation failed to reverse TRPV1-mediated inhibition of EGFR signaling in both HCT116 (**left panel**) and CHO cells (**right panel**). **(C)** Validation of FK506 as a potent inhibitor

of the Ser phosphatase activity of calcineurin in HCT116 cells. Cells were pretreated with 0, 1, or 10 μM FK506 (1 hr), followed by stimulation with or without 5 μM ionomycin (30 min). Total cell lysates were analyzed for calcineurin target, NFAT1, by using antibodies that recognize total and phosphorylated NFAT1. **(D)** Calcineurin inhibitor, FK506 (10 μM), did not reverse the inhibition of EGFR phosphorylation by TRPV1. The same experimental approach was applied with HCT116 and CHO cells, respectively, as in **B**. **(E)** Quantification of expression levels of PTP candidates in WT versus *Trpv1*$^{-/-}$ colon crypts by Q-PCR, normalized for *Gapdh*. Results are shown as mean ± SEM. **(F)** Dephosphorylation of PTP1B target Hrs in TRPV1 overexpressing cells. HCT116 cells were transfected with empty vector or TRPV1 plasmid. Two days later, cells were stimulated with EGF (1 ng/mL) for indicated time periods, followed by Western blot analysis with antibodies directed to phospho-EGFR^{Y1068}, total EGFR, phospho-Hrs^{Y334}, or β-actin. **(G)** Transfection of HCT116 cells wirh empty vector, WT PTP1B (PTP435), or PTP1B truncation mutants (PTP370, PTP377). Total cell lysates were analyzed by IB with anti-HA tag mAbs. **(H)** Validation of IEC fractionation. Q-PCR analysis showed enrichment for *Lgr5*, *Mmp7*, and *Egr1* in the crypt fraction (normalized for *Gapdh*). Conversely, mature enterocyte marker *Slc26a3* (a chloride anion exchanger) expression was relatively enriched in villus fractions. Data are mean ± SEM (n=3/group).

Supplemental Figure 7. Functional association between TRPV1 and EGFR signaling pathways. **(A)** Validation of PLCγ1 knockdown in control and *PLCG1* siRNA transfected cells by Western blotting. **(B)** Model for the triggering of TRPV1 by EGFR, as explained in text. DAG, diacylglycerol; IP_3, inositol trisphosphate; PIP_2, phosphatidylinositol-4,5-bisphosphate; PLC, phospholipase C.

Supplemental Figure 8. TRPV1 deficiency on the *Apc$^{min/+}$* background. (A) Enhanced expression of *c-Fos* mRNA in mice with hetero- or homozygous deletion of *Trpv1* on the Min background as determined by PCR. **(B)** Increased expression of *c-Fos* in *Apc$^{min/+}$/Trpv1$^{+/-}$* (wt/ko) and *Apc$^{min/+}$/Trpv1$^{-/-}$* (ko/ko), compared to *Apc$^{min/+}$/Trpv1$^{+/+}$* (wt/wt) mice. Q-PCR was performed with IEC lysates from age-matched mice and data were normalized for *Gapdh*. **(C)** Systemic ablation of TRPV1+ sensory neurons in *Apc$^{min/+}$* mice did not recapitulate the phenotype of *Apc$^{min/+}$/Trpv1$^{-/-}$* mice. *Apc$^{min/+}$* mice were treated with 50 μg/kg resiniferatoxin (RTX) s.c. on day 1, 2, and 7 after birth. Ablation of TRPV1+ neurons was validated by a negative eye wipe test by ocular challenge with 0.01% (w/v) capsaicin in saline between 6-8 weeks. The cohort of *Apc$^{min/+}$* mice (n=16) is the same as shown in **Figure 7D** for direct comparison with *Apc$^{min/+}$* RTX mice (n=11). Median survival of *Apc$^{min/+}$* (control) and *Apc$^{min/+}$* RTX mice were 23.2 and 24 weeks, respectively. **P*=0.0397 (Log-rank test). **(D) Left panel:** Polyp counts (>1 mm) of *Apc$^{min/+}$* (control) and *Apc$^{min/+}$* RTX mice (n=12 and n=11, respectively). Control cohort is the same as shown in **Figure 7B**. **Right panel:** Hemoglobin levels of control and RTX-treated *Apc$^{min/+}$* mice (n=10 and n=18, respectively) at 20 weeks. Control cohort is the same as shown in **Figure 7C**.

Supplemental Figure 9. TRPV1 vs. TRPV5 in the regulation of the EGFR. The proposed mechanism of TRPV1-mediated feedback on EGFR signaling, which is initiated by PLCγ activation and PIP_2 depletion. This mechanism is likely distinct from that mediated by TRPV5.

Supplemental Tables

Supplemental Table 1: Mouse primers.

Gene	Official full name	Accession No.	Sequence 5'-3'
Axin2	axin2	NM_015732.4	CAGTGAGCTGGTTGTCACCT CTGAGCTGCTCCTTGAAGTG
c-Fos	FBJ osteosarcoma oncogene	NM_010234.2	ACCATGATGTTCTCGGGTTTC GCTGGTGGAGATGGCTGTCAC
c-Jun	Jun oncogene	NM_010591	GCAGAAAGTCATGAACCACG GCAACCAGTCAAGTTCTCAAG
c-Myc	myelocytomatosis oncogene	NM_001177353.1 NM_010849.4	TGGTGTCTGTGGAGAAGAGGCAAA TTGGCAGCTGGATAGTCCTTCCTT
Cldn6	claudin 6	NM_018777.4	GGATGTCCTGTGTGGTTCAG AGGACAATGAGGAGGGTGAC
Egr1	early growth response 1	NM_007913	GTGTGCCCTCAGTAGCTTC GACATCAATTGCATCTCGGC
Fosl2 (Fra-2)	fos-like antigen 2	NM_008037.4	CGGGAACTTTGACACCTCG TGATGGCGTTGATTGTGGG
Gapdh	glyceraldehyde-3-phosphate dehydrogenase	NM_008084	TCAACAGCAACTCCCACTCTT ACCCTGTTGCTGTAGCCGTAT
Lgr5	leucine rich repeat containing G protein coupled receptor 5	NM_010195.2	TGAGCGGGACCTTGAAGATTTCCT AGCCAGCTACCAAATAGGTGCTCA
Mki67	antigen identified by monoclonal antibody Ki 67	NM_001081117.2	TGCCCGACCCTACAAAATG GAGCCTGTATCACTCATCTGC
Mmp7	matrix metallopeptidase 7	NM_010810	AACACTCTAGGTCATGCCTTCGCA AGACCCAGAGAGTGGCCAAATTCA
Nefl	neurofilament, light	NM_010910	GGCCTTGGACATCGAGATTG

	polypeptide		TCTGCAAGCCACTGTAAGC
Ocln	occludin	NM_008756.2	TCCACACTCAAGGTCAGAGG CAATGGCCTACTCCTCCAAT
Slc26a3	solute carrier family 26, member 3	NM_021353.3	AGGGAATGCTGATGCAGTTTGCTG AGTTGAAATGCTACACTTGCCGCC
Trpv1	transient receptor potential cation channel, subfamily V, member 1	NM_001001445	AGCTGCAGCGAGCCATCACCA ATCCTTGCCGTCCGGCGTGA
Trpv2	transient receptor potential cation channel, subfamily V, member 2	NM_011706	CCAGCCATTCCCTCATCAAAA AAGTACCACAGCTGGCCCAGTA
Trpv3	transient receptor potential cation channel, subfamily V, member 3	NM_145099	TGAAAGAAGGCATTGCCATTT GAAACCAGGCATCTGACAGGAT
Trpv4	transient receptor potential cation channel, subfamily V, member 4	NM_022017	TCACCTTCGTGCTCCTGTTG AGATGTGCTTGCTCTCCTTG
Trpv5	transient receptor potential cation channel, subfamily V, member 5	NM_001007572	CGTTGGTTCTTACGGGTTGAAC GTTTGGAGAACCACAGAGCCTCTA
Trpv6	transient receptor potential cation channel, subfamily V, member 6	NM_022413	ATCCGCCGCTATGCACA AGTTTTTCTCCTGAATCTTTTTCCA

Supplemental Table 2: Other primers.

Gene	Accession number	Sequence 5'-3'
hGAPDH	NM_002046.3	ACCAAATCCGTTGACTCCGAC TTCGACAGTCAGCCGCATCT
hTRPV1	NM_080704.3 NM_018727.5 NM_080706.3 NM_080705.3	TGGATGGCTTGCCTCCCTTTA ACTGTAGCTGTCCACAAACAG
CRE	B449974.1	TCCATATTGGCAGAAGGAA CAGCTACACCAGAGACGGAA

Supplemental Figure 1

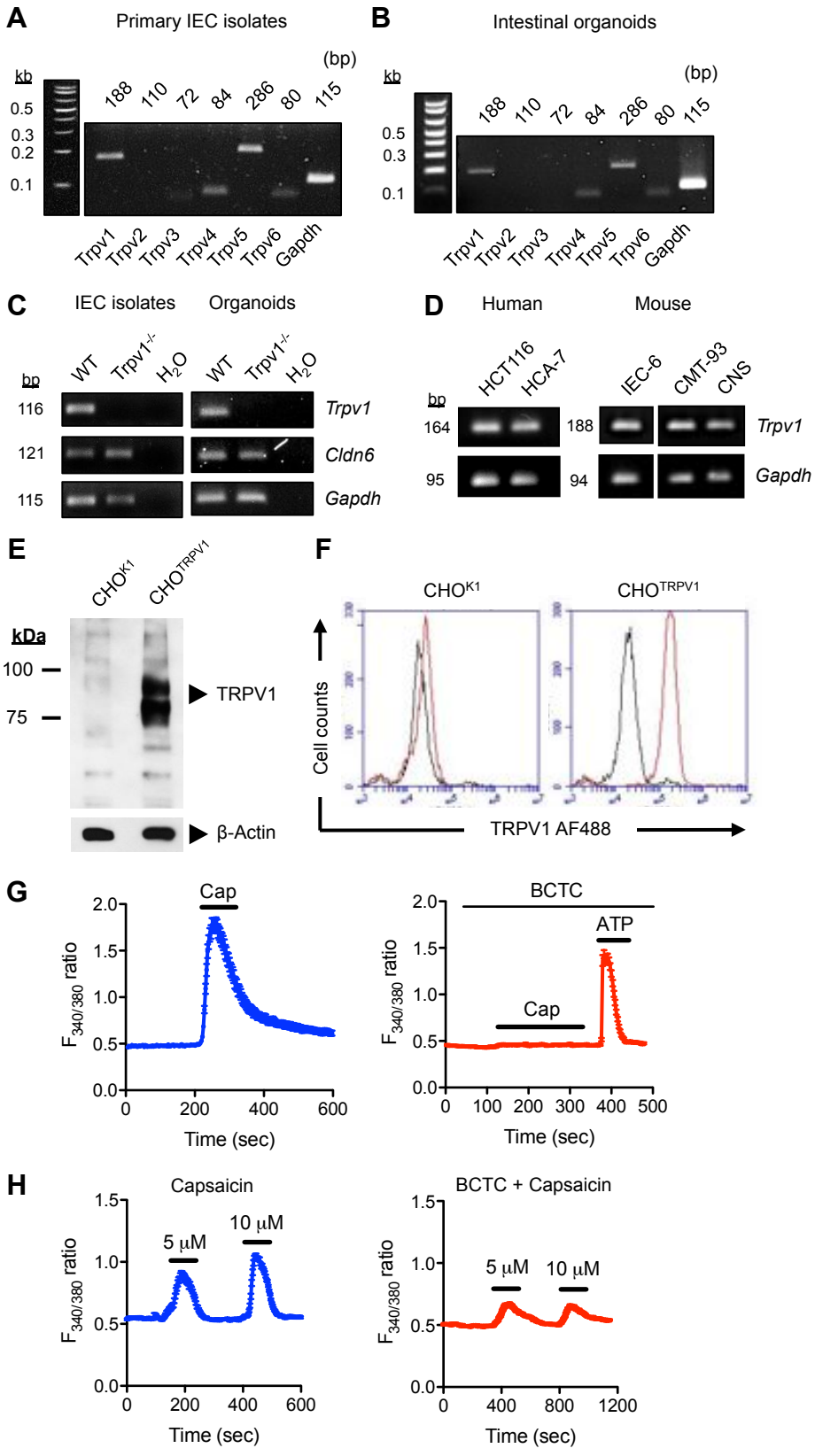

Supplemental Figure 2

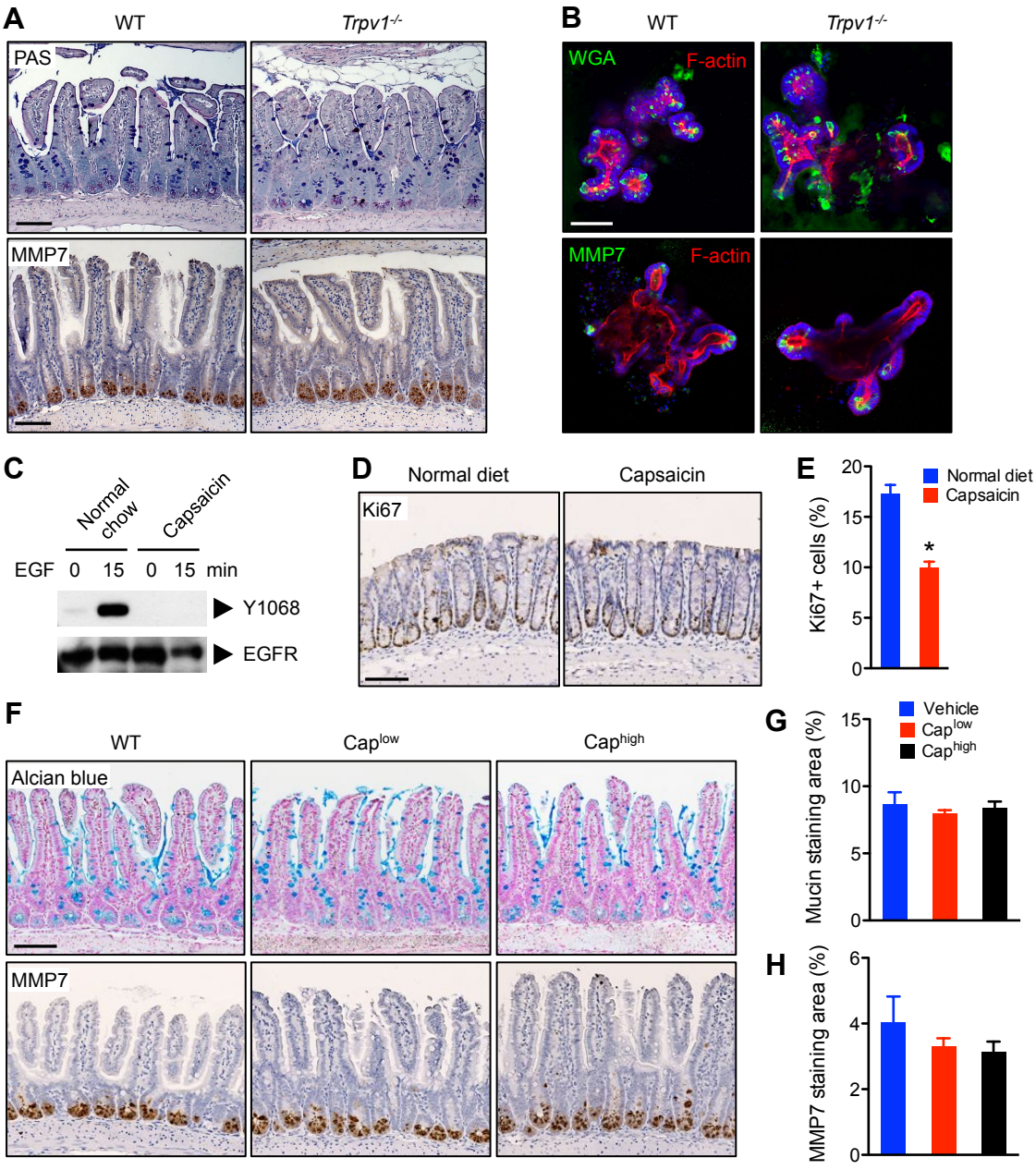

Supplemental Figure 3

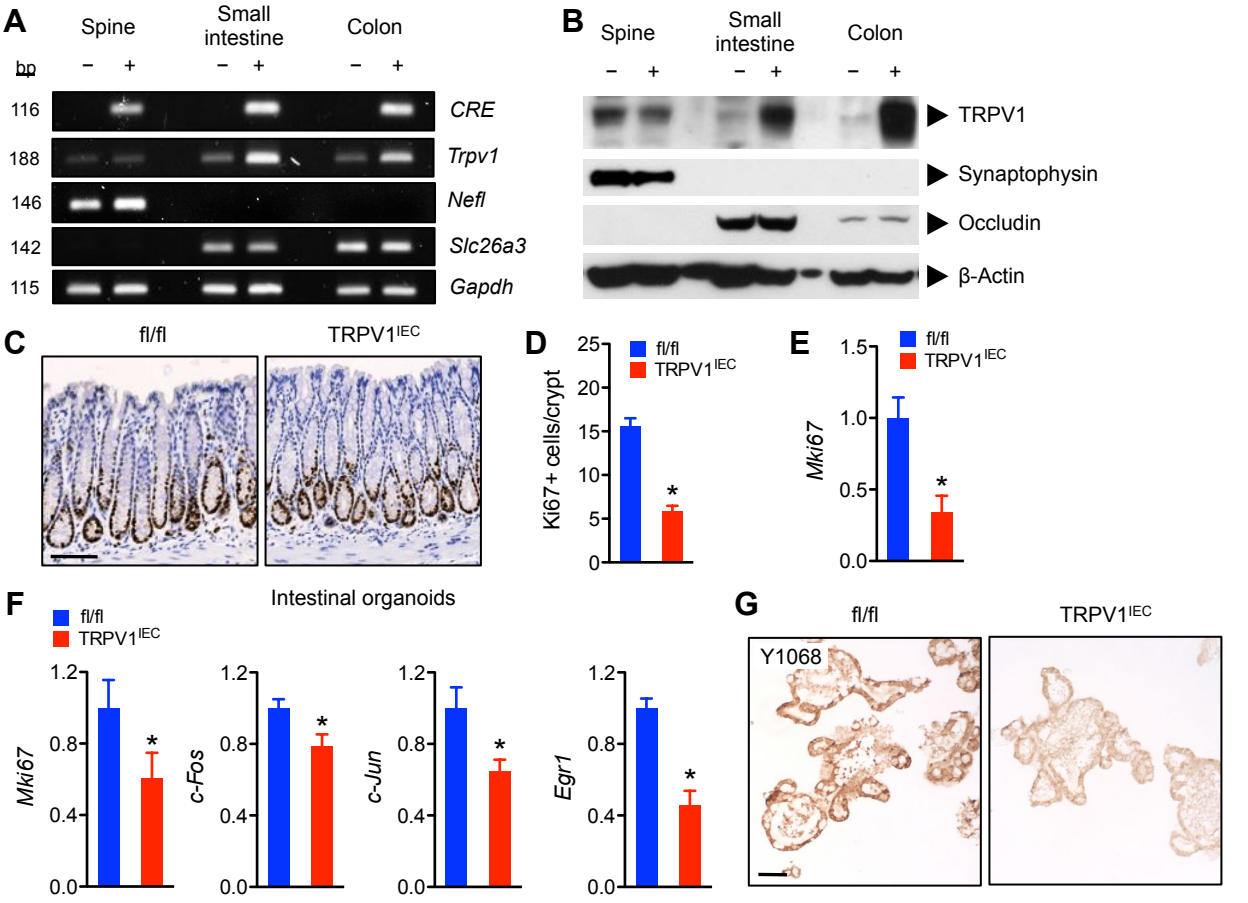

Supplemental Figure 4

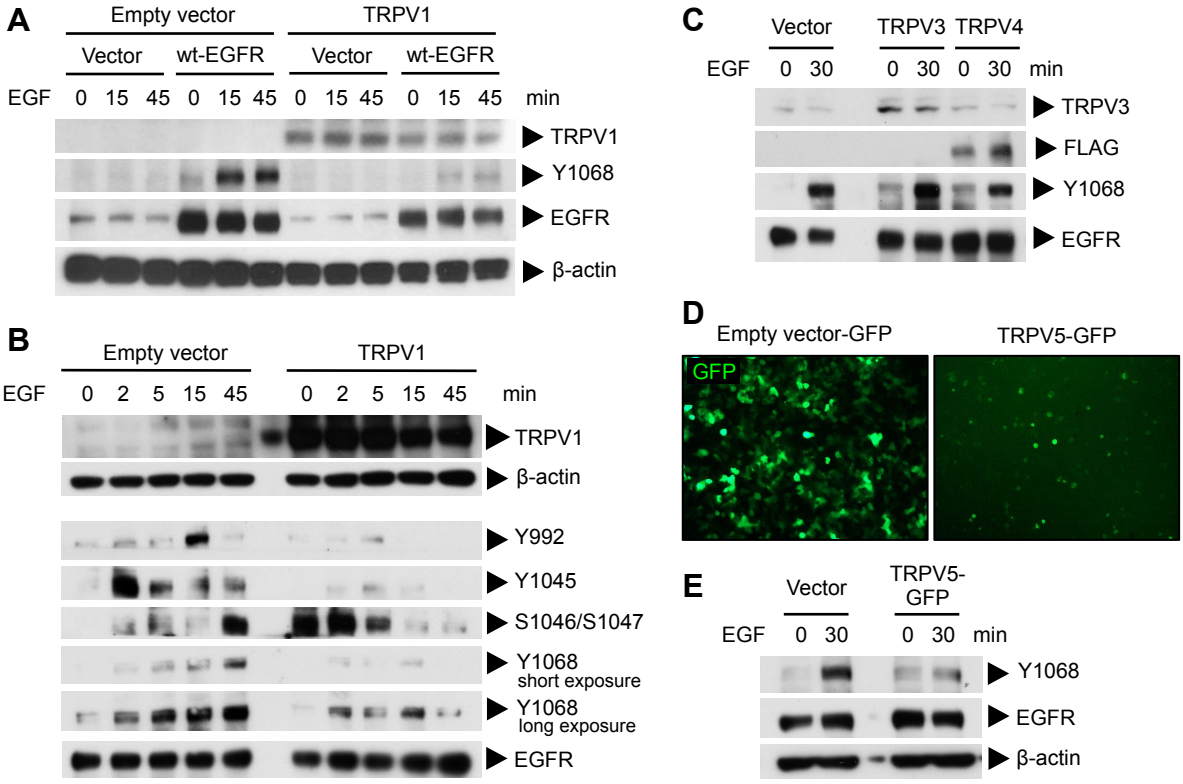

Supplemental Figure 5

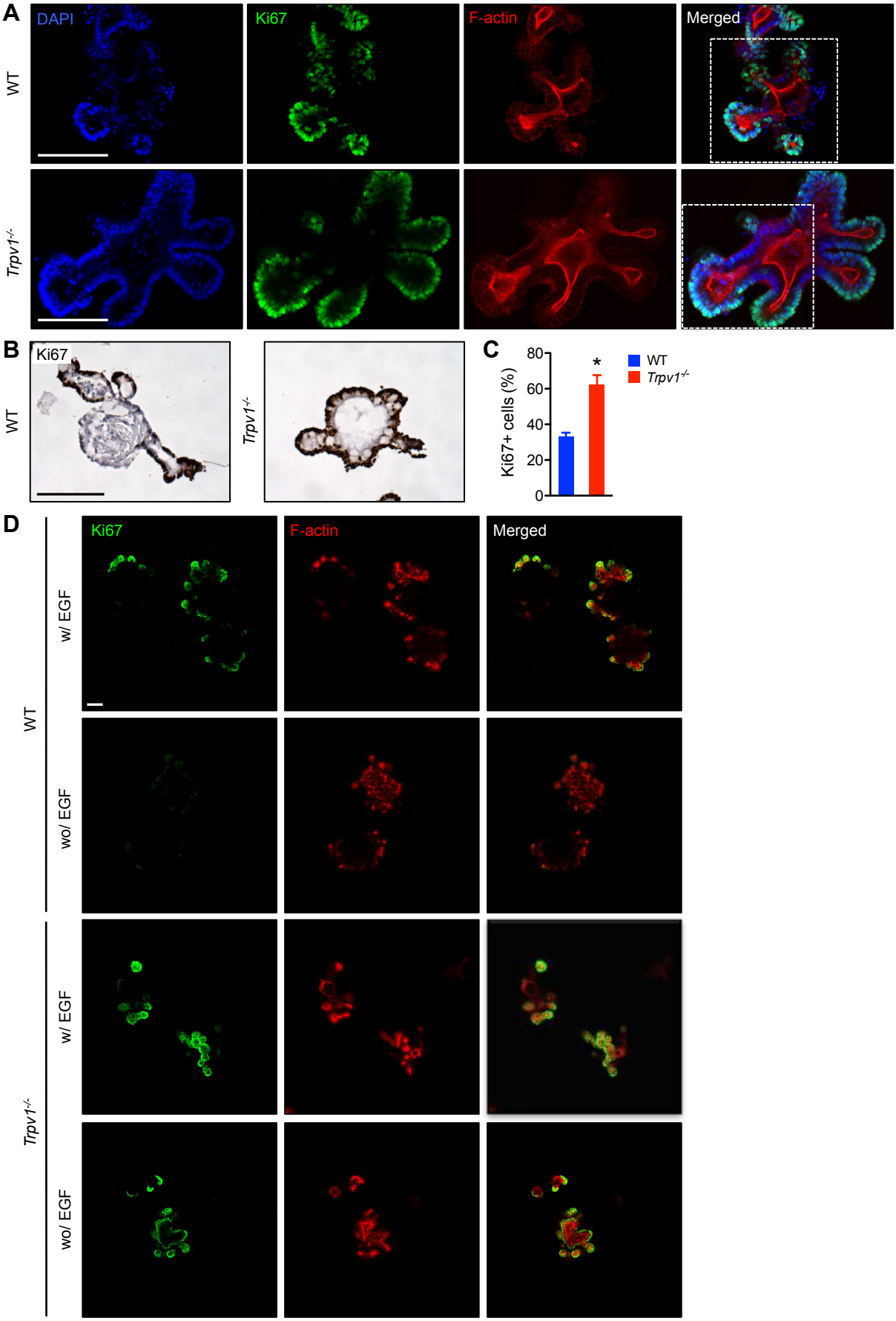

Supplemental Figure 6

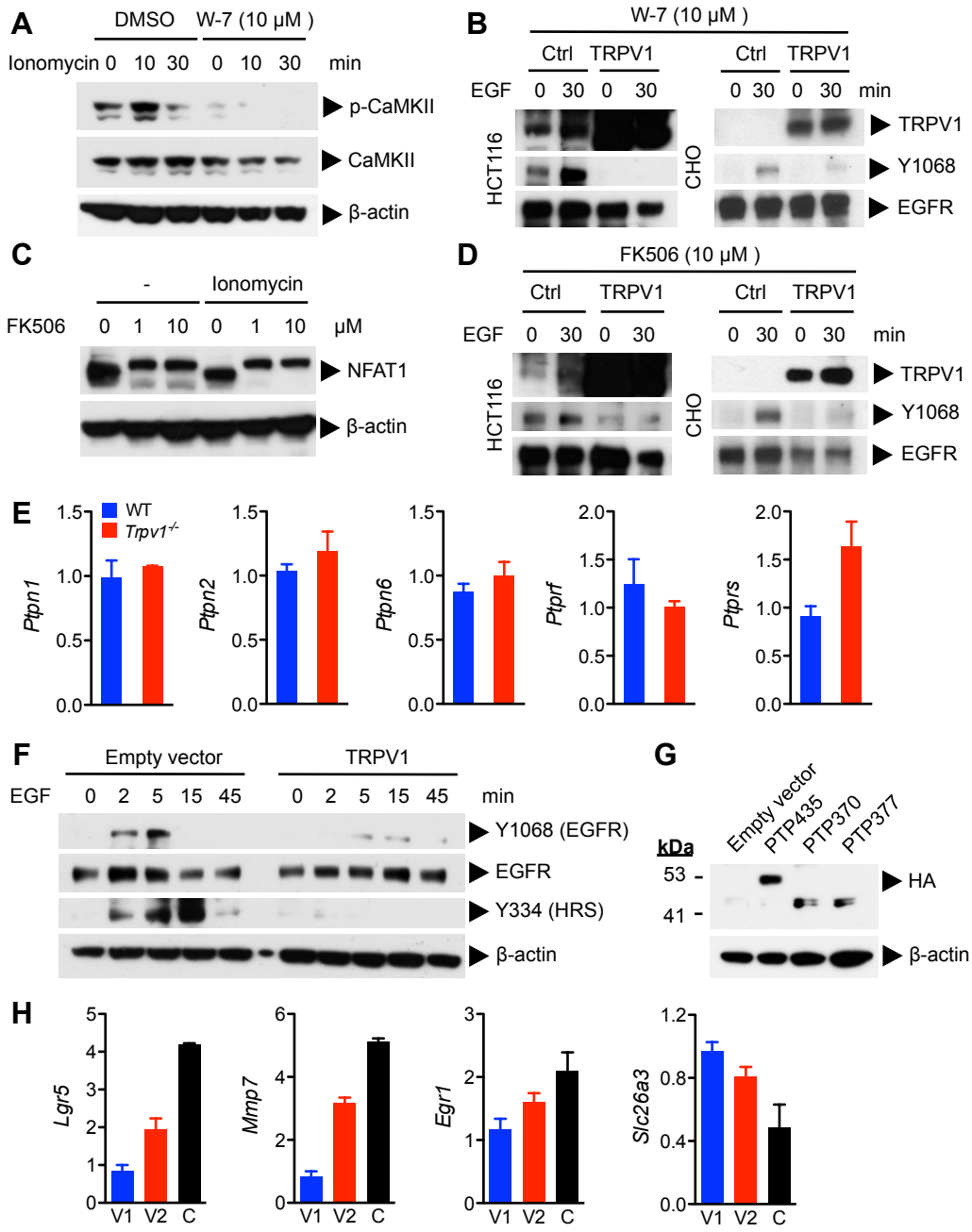

Supplemental Figure 7

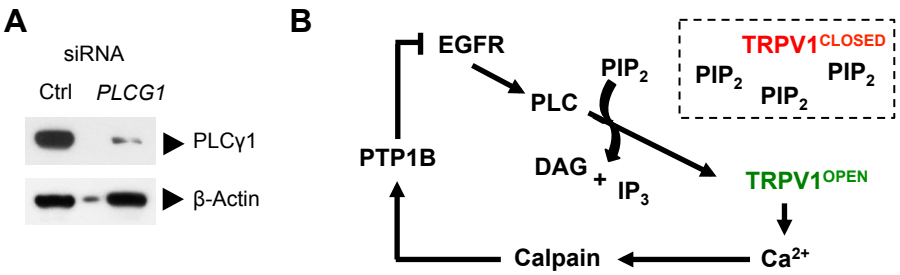

Supplemental Figure 8

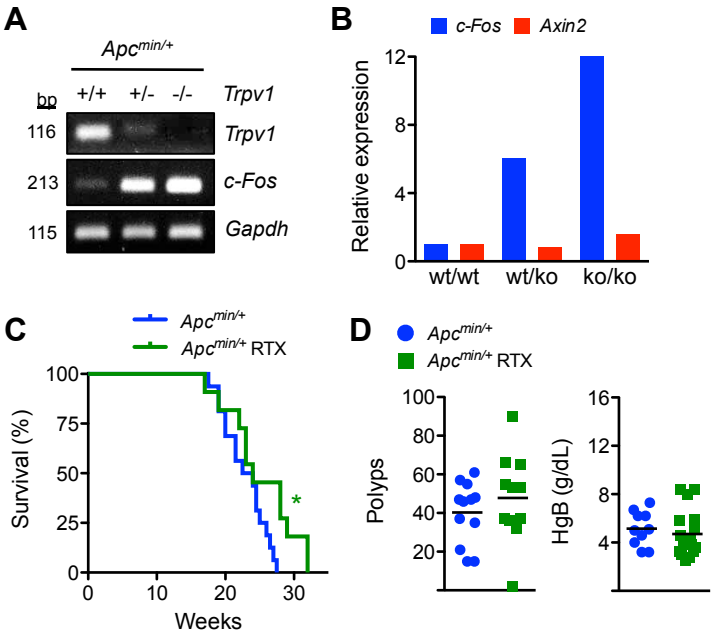

Supplemental Figure 9